
Bachelor's Project

TRANSMONS: BENCHMARKING GATE CONTROL

Author	Michael Spange Olsen
Advisor	Charles Marcus
Co-Advisor	Karl Petersson

Center for
Quantum
Devices



Gruppe

Center for Quantum Devices

Submitted to:

The Niels Bohr Institute, University of Copenhagen

June 10, 2015

swedish license plate: xqc743

ACKNOWLEDGEMENTS

First of all i would like to say thank you to the Transmonteam, to Charlie and everyone in the lab for being so welcoming. It has been a joy to be around (though sometimes frustrating when the equipment wont do, what you want them to).

Espicially thanks to Karl my supervisor. You have been incredibly patient, and i've had a good time working with you.

I would also like to thank Thorvald whom has taugh me a *LOT!* Thx for being so understanding and taking your time introducing me to the whole thing!

Lucas i would also like to thank: It has been Great working with you - though it sometimes has been some long days, and nights, in the lab.

Last but not least, I am grateful towards Charlie to let me work at his lab, and i look forward to further collaboration - please bear with me for some time.

CONTENTS

1	Introduction	1
2	Theory	3
2.1	Qubits	3
2.1.1	Superconducting qubits	3
2.1.2	Cooper-Pair Box	4
2.1.3	Gatemon	5
2.2	cQED (dispersive regime)	6
2.3	Single qubit gate rotations	7
2.3.1	Tuning	7
2.4	Clifford Benchmarking: gate errors	9
3	Setup	13
3.1	Dilution fridge	13
3.2	Wiring and control electronics	14
3.3	Qubit device	15
4	Data	17
4.1	Single qubit control (with microwaves)	17
4.2	Randomized benchmarking	19
5	Conclusion and Outlook	21
A	Appendix	23
	Bibliography	25

ABSTRACT

The use of nano wires in the Josephson junction in superconducting circuit introduces some great advantages, such as voltage controlled Josephson energies without the need of any currents.

In this thesis i use random benchmarking as an indicator of the progress towards fault tolerant computing. I show how we are as close one can be, with only a 1/2 to a 1 procent of uncertainty between us and certainty.

INTRODUCTION

IN classical computing, bits in states of either 0 or 1 are used as the foundation. Similar, quantum computing uses the same logical build up, However using the superposition principle, we create a bit, that can be in a superposition between 0 and 1. A qubit.

Quantum computing holds great potential, since it was proposed, and the concept of solving problems using quantum algorithms. Computational task are sped up moderately, quadratically and even exponentially. We even have new task that are not doable in classical computers, like quantum cryptography [1].

Now we just need to get to the point where we can do quantum computations. Well there are hurdles. The one i will concentrate one is, if to be able to do quantum computing, we need fault tolerant quantum circuits. In order to create these fault tolerant circuits, the building block, the single qubit, must have a threshold fidelity. Below the fidelity, the qubits will induce to many errors, and information will be lost. We require only 99% fidelity gates per step.[2]

In order to gauge the fidelity of our qubits, i focus on doing random benchmarking on our system. Our system being the recently newly developed gatemon [7].

In this thesis, I will first go through the qubit itself, and the basics of the system. Then I move on to the readout and control of the qubit, before giving the background for the random benchmarking. I'll then very briefly touch upon the instruments we are using and then move on to the main subject; random benchmarking using a set of gates called a Clifford group. Here the first results of this endeavour, on the relatively

new and promising gatemon qubits will be presented in the end.

2.1 Qubits



THE gatemon used in this thesis is a trasmon-like superconducting qubit [7].

2.1.1 Superconducting qubits

With superconducting circuit elements, we can get circuits with low loss, and with a simple lossless parallel LC resonator, we get a perfect harmonic oscillator. If we have this at very low temperatures, with the harmonic energy $\hbar\omega \ll k_B T$, and thus in the ground state, we can apply pulses at the resonant frequency to drive the transition between the ground state and the first excited state. However, due to the even spacing of the harmonic oscillator, this pulse will drive all the degenerated energy-levels. To get around this we use a non-linear circuit element: the Josephson junction. The Josephson junction is two superconducting layers, separated by a thin

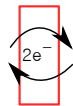


Figure 2.1: Josephson junction. Two superconducting layers are separated by a non-superconducting layer. The phase difference between the two layers giving rise to Cooper-pair tunnelling

barrier (Fig 2.1). This has a supercurrent I across the barrier, given by[5].

$$I = I_0 \sin(\phi(t)) \quad (2.1)$$

Where I_0 is the maximum zero-voltage current, the critical current, and $\phi(t)$ is the phase difference across the junction, evolving in time in the presence of a potential V . Taking e as the electron charge, ϕ is then given by

$$\hbar \frac{d\phi}{dt} = 2eV \quad (2.2)$$

By differentiating 2.1 and using that the inductance is given by $V = L\dot{I}$ we get the non-linear Josephson inductance L_J

$$L_J = \frac{\hbar}{I_0 e \cos(\phi)} \quad (2.3)$$

Since the Josephson junction is two separated layers, it also has an intrinsic capacitance, given by C_J . The Josephson junction is then a non-linear LC circuit, which might allow for selective transitions between ground state and first excited state.

2.1.2 Cooper-Pair Box

A simple way to use a Josephson Junction is to connect one of the superconducting layers with a reservoir of Cooper-pairs, leaving the other part of the junction as an superconducting island. Moreover, if the total island capacitance, C_Σ , is sufficiently small, one can induce Coulomb blockade of tunnelling, and we have the Cooper-Pair Box. This system has the Hamiltonian

$$H = 4E_C(\hat{n} - n_g)^2 - E_J \cos(\phi) \quad (2.4)$$

Here $E_C = e^2/2C_\Sigma$, is a 'charging' energy, with $C_\Sigma = \Sigma C_i$, the sum of capacitance to ground. $E_J = I_0\hbar/2e$ is the Josephson Energy, $(\hat{n} - n_g)$ is the Cooper-Pair operator counting the number of Cooper-Pairs above the ground state. Here the offset is controlled by an external gate voltage.

The transmon qubit comes into play, in order to fight $1/f$ charge noise. The ratio of E_J/E_C determines the relative anharmonicity, with decreasing anharmonicity for increasing ratios of E_J/E_C . Furthermore, charge noise sensitivity in the system is reduced with increasing ratios of

E_J/E_C . However, it is not just sweet lullabies, since the qubit operation speed is decreased [6].

The transmon utilizes the fact that even though we lose anharmonicity and thus operation speed, we do so algebraically to a low power, while we reduce the charge dispersion exponentially.[6]

When operating in the $E_J \ll E_C$ regime (transmon regime), the system is best described as an anharmonic oscillator, with an absolute anharmonicity $\alpha_m \cong -E_C$. The absolute anharmonicity described by the difference in the transition energy between the m to $(m + 1)$ energy level, and the m to $(m - 1)$ energy level. $2E_m - E_{m+1} - E_{m-1}$ Comparing α_m to the transition energy between ground and first excited state, $E_{01} \cong \sqrt{8E_J E_C}$, gives us the relative anharmonicity

$$\alpha_m^r = -\sqrt{\frac{E_C}{8E_J}} \quad (2.5)$$

This shows the algebraic decrease in anharmonicity with an increasing E_J/E_C . However, up till now E_J has been purely fixed by the design. To be able to tune E_J we must introduce more to the design.

2.1.3 Gatemon

There are different ways to introduce this tuneability. In multiple other Transmon experiments, the tuneability is introduced by adding two junctions in parallel in a so called SQUID-design. This gives a magnetic flux dependent $E_J(\Theta)$. [3][9] However, to introduce a flux, a current through a coil is needed, thus potentially depositing energy in the fridge. In these designs currents on the scale of mA are needed, in order to thread one flux quantum. For small numbers of qubits this has not been a problem so far. For large numbers of qubits, as needed for a big quantum processor, sending down hundreds of mA into a mK environment is potentially a problem.

To get around this problem, the Gatemon was introduced[7] This qubit is a Transmon, using a superconductor-semiconductor-superconductor(SNS) interface as a Josephson junction. The carrier density within the semiconductor can be controlled by a electrostatic field, and therefore also the coupling to the superconductors. Only needing a electrostatic field, no current is needed, thus getting around that particular scaling problem. More specifically InAs-Al nanowires are used in the design used in this thesis. The superconducting Aluminium is etched away for a small region, creating the Josephson junction. Bringing in close a voltage gate, then

gives a aperiodic voltage dependent $E_J(V_g)$. The aperiodic fluctuations are associated with fluctuations in the nanowire[7].

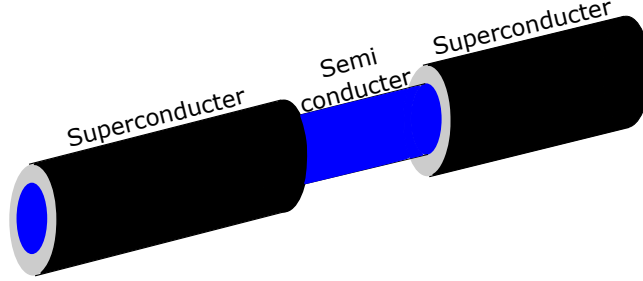


Figure 2.2: The nanowire Josephson junction of the Gatemon. And area of the superconductor is etched away, forming the tunable gap.

2.2 cQED (dispersive regime)

IN ORDER to measure on the two-level system that is the gatemon, we can couple the qubit to the surroundings, using circuit quantum electrodynamics (cQED). As in atomic physics were an atom is coupled to a cavity with a coupling strength g , we couple a superconducting qubit ('atom') with a superconducting resonator (in a lossless environment, a perfect harmonic oscillator) ('cavity'). Seeing the qubit as a two-level system, we can then model the system using the Jaynes-Cummings Hamiltonian[9].

$$H_{JC} = \hbar\omega_c(a^\dagger a + 1/2) + \hbar\frac{\omega_q}{2}\sigma_z + \hbar g(a^\dagger\sigma^- + a\sigma^+) \quad (2.6)$$

with the bare cavity frequency $f_c = \omega_c/2\pi$, qubit frequency $f_q = \omega_q/2\pi$, the coupling strength g , a^\dagger/a the creation/annihilation operator of the harmonic oscillator, σ_z is the qubit operator, and the interaction between qubit and cavity where the qubit absorbs ($a\sigma^+$) or emits ($a^\dagger\sigma^-$) an energy quantum.

If the qubit and cavity is in the resonant limit ($\omega_q - \omega_c \ll g$), the eigenstates of the system is a superposition between qubit and cavity eigenstates, effectively making it a strongly coupled system, were the individual characteristics of the cavity and the qubit are blurred.

Instead we want the the interaction to be dispersive limit, where we detune the cavity and the qubit, such that $\omega_q - \omega_c = \Delta \gg g$. In this limit,

no energy is exchanged between the qubit and the cavity. In the dispersive regime, the Hamiltonian can be approximated to

$$H_{JC\text{-dispersive}} = \frac{1}{2}\hbar\omega_q\sigma_z + \hbar\left(\omega_c + \frac{g^2}{\Delta}\sigma_z\right)\left(a^\dagger a + \frac{1}{2}\right) \quad (2.7)$$

Looking at the cavity-term, the interaction with the qubit, has caused a shift in frequency, dependent on the qubit state. Whether or not the qubit is in the $|0\rangle$ or $|1\rangle$ state, the cavity is shifted by $2g^2/\Delta$. Thus probing the cavity can reveal what state the qubit is in. The most important part, is though, that this probing method is a quantum non-demolition measurement. This means, that we can probe the state of the qubit, without destroying it. Instead, the qubit is projected into one of its eigenstates, and within the qubit lifetime, we are able to measure the same value repeatedly, and thereby gain better readout fidelity.[9][10].

2.3 Single qubit gate rotations

ONTROL of the qubit is utilized with microwave pulses. Since we want a qubit comprised of only two states, we can express those as $|0\rangle$ and $|1\rangle$, all gates we apply should make the qubit travel only in the Hilbert space spanned by these two states. Since we can span the whole subspace, from pure $|0\rangle$ and $|1\rangle$ states, to different superpositions such as $\frac{|0\rangle+|1\rangle}{\sqrt{2}}$ and $\frac{|0\rangle-i|1\rangle}{\sqrt{2}}$. This subspace, we can represent on a Bloch-sphere (Fig [2.3]). However we do only want to access the 6 states that are eigenstates of the Pauli matrices.:

$$|0\rangle, |1\rangle, \frac{|0\rangle + |1\rangle}{\sqrt{2}}, \frac{|0\rangle - |1\rangle}{\sqrt{2}}, \frac{|0\rangle + i|1\rangle}{\sqrt{2}}, \frac{|0\rangle - i|1\rangle}{\sqrt{2}} \quad (2.8)$$

Using pulses we can reach the whole Bloch sphere, with arbitrary rotations. In practice we don't use the all the arbitrary rotations available, but rather only the π and $\pi/2$ rotations about the z, x and y axis. The z-axis we are able to swap with x and y control for the one qubit control. This is often the simplest, and are all we need to build up the single qubit Clifford group, that will be discussed later.

2.3.1 Tuning

The Frequency is tuned two ways. Coarse qubit spectroscopy by just measuring the cavity response when sweeping the qubit drive frequency.

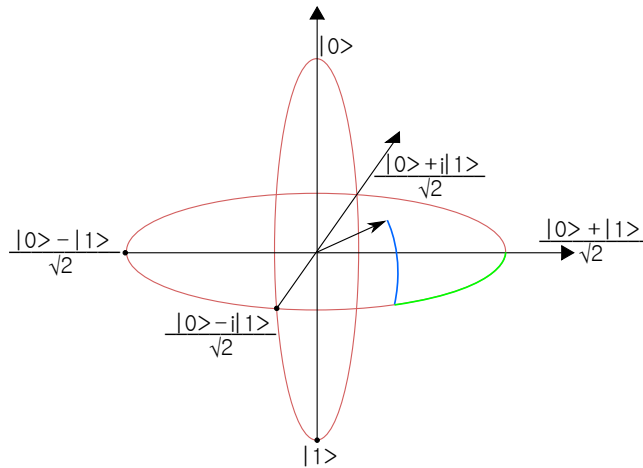


Figure 2.3: Bloch sphere representing the Hilbert space spanned by $|0\rangle$ and $|1\rangle$, that is available through qubit manipulation. The three Pauli matrices can then generate rotations around the three axes; x , y and z . The state of the qubit is fully described by only two numbers: the polar angle θ and the azimuthal angle ϕ

Due to Eq. 2.7, there will be a shift of $2g^2/\Delta$ in the cavity frequency, and thus also a response in the magnitude and phase of the cavity readout. This however has its limitations, due to power broadening and pulse bandwidth[8].

Instead, a Ramsey experiment can be utilized to gauge the frequency to much higher precision. Ramsey oscillations utilize the fact that for a finite angular frequency detuning Δ of the qubit from resonance, the phase evolves as $\phi = \Delta * t$. By bringing the qubit onto the equator, wait a time t , and then apply a second similar pulse, the qubit will oscillate between $|0\rangle$ and $|1\rangle$ state with a angular frequency of Δ . This measurement of the frequency will be limited only by the dephasing rate.

In order to get the π and $\pi/2$ pulses calibrated, Rabi oscillations are carried out. Rabi oscillations is the name for the continues rotation around the Bloch sphere for long control pulses. When applying pulses of constant power, at a continuously longer time, the qubit is going to oscillate between being in the $|0\rangle$ and the $|1\rangle$ state. Likewise when applying pulses with a fixed pulse width, and sweeping the power.

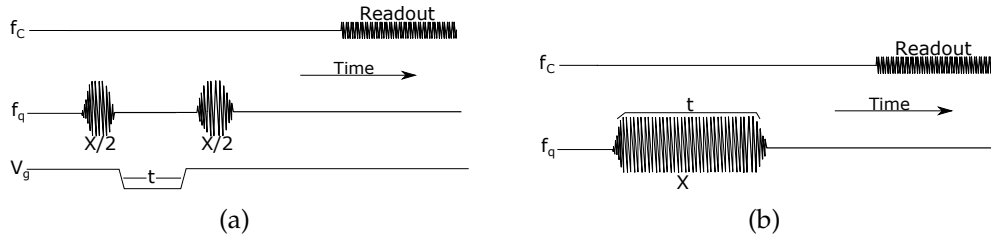


Figure 2.4: (a) Ramsey experiment. A $\pi/2$ pulse is followed by a waiting time of t , during which a pulse is applied to the gate, bringing the qubit out of resonance. After t time, a second $\pi/2$ pulse gives the qubit a phasedependent qubit rotation. (b) Rabi oscillations performed by varying the pulsetime. The pulse just keeps the qubit oscillating around in the Bloch sphere frame.

2.4 Clifford Benchmarking: gate errors

To quantify the errors on the different gate operations, we use random benchmarking[4]. In order to make a random benchmarking, we need a set of qubit-rotations, that covers all the points, on the Bloch sphere that we are using, evenly (Eq. 2.8)[2].

Since we have 6 states, and a rotation symmetry of 4 - we need 24 different qubit operations in order to cover all rotations. These 24 qubit operations will then be the full Clifford set. Writing the π rotations as X and Y, the $\pi/2$ rotations as X/2 and Y/2 and the identity operation as I, the 24 Clifford gates are:

- | | |
|---------------|--------------------|
| 1. I | 2. -Y/2, X/2 |
| 1. X | 2. -Y/2, -X/2 |
| 1. Y | 3. X/2 |
| 1. Y, X | 3. -X/2 |
| 2. X/2, Y/2 | 3. Y/2 |
| 2. X/2, -Y/2 | 3. -Y/2 |
| 2. -X/2, Y/2 | 3. -X/2, Y/2, X/2 |
| 2. -X/2, -Y/2 | 3. -X/2, -Y/2, X/2 |
| 2. Y/2, X/2 | 4. X, Y/2 |
| 2. Y/2, -X/2 | 4. X, -Y/2 |

4. $Y, X/2$ 4. $X/2, Y/2, X/2$ 4. $Y, -X/2$ 4. $-X/2, Y/2, -X/2$

The first group are Pauli rotations. The second group is $2\pi/3$ rotations, as three uses of the same gate is the identity operator. The Third group consists of $\pi/2$ rotations, and the fourth group of Hadamard-like rotations[2]. All the Hadamard-like rotations return the qubit to the initial state when used twice.

Because some of the Clifford gates consist of single qubit gates, the average single qubit gate per Clifford gate is

$$\frac{\sum(\text{single qubit gates})}{\sum(\text{Clifford gates})} = 1.875 \quad (2.9)$$

The important thing about Clifford gates is, that they cover the Bloch sphere evenly, thus a sequence averages over errors from all gates. At the same time, we can probe the errors on each gate separately. To gain knowledge about the error on a specific gate, that specific gate is interleaved in a random Clifford sequence. From the error on non-interleaved Clifford sequences, it is possible to extract the error on the individual gate.

We are interested in the errors on the gates, in order to fight them. The Clifford gates are quantum computational gates, and to implement e.g. fault tolerant surface code, a certain fidelity threshold is needed [2]. The random benchmarking gives us the means to gauge how far we've come.

The reference is generated by doing random Clifford sequences of m Clifford gates, and in the end do a pulse to revert the qubit to ground state. Errors will then be evident, when the measured cavity response differs from the ground state value. This value can be calibrated by doing a Rabi measurement, measuring the cavity response when in the ground state, and the first excited state. The reference sequence fidelity F_{ref} then follows an exponential law

$$F_{ref} = Ap_{ref}^m + B \quad (2.10)$$

where p_{ref} is the decay of the sequence, and A and B will capture errors in e.g. state preparation and measurement. The average gate reference error is then given by

$$r_{ref} = \frac{1 - p_{ref}}{2} \quad (2.11)$$

When we now interleave gates, we can then use the p_{ref} together with p_{gate} to find the gate error

$$r_{gate} = \frac{1 - p_{gate}/p_{ref}}{2} \quad (2.12)$$

$$\begin{array}{l} \text{Reference} \quad \left(C \right)^m - C_r - \text{pulse} \\ \text{Interleaved } G \left(C - G \right)^m - C_r - \text{pulse} \end{array}$$

Figure 2.5: Building up a random Clifford sequence of m gates, as a reference. Building the sequence for the interleaved gates is equal, only after each random Clifford gate, we insert the chosen gate G . Both sequences are ended with a pulse returning the qubit to the ground state before it is measured.

THE EXPERIMENTAL SETUP

3.1 Dilution fridge

IN order to get to the ground state of the system, we need a very cold environment. We use a Cryofree Dilution Refrigerator from Oxford instruments. These fridges can produce mK cold environment by circulating ^3He through several heat exchangers on its way down to the final level, where it is mixed with superfluid ^4He . When the condensed ^3He is mixed with the superfluid ^4He , only a small amount is mixed. Instead a phase boundary between ^4He -rich and ^3He -rich occurs. By removing the small amount of ^3He in the ^4He rich part, forces some of the ^3He to cross the phase boundary, which costs energy. This energy is taking from the surroundings effectively cooling the fridge down to a few tens of mK .

To load the sample inside the fridge, we mount them inside a 'puck', see Fig 3.1. The inside of the puck has been painted with special paint that gives magnetic shielding. Also a magnetic shield has been installed, being a long tube that sits inside the fridge, just around the loaded puck. The hope being that it might reduce some of the frequency sliding seen earlier in the samples. No test of whether it has helped or not, have been made.



Figure 3.1: The puck used to load the sample. The yellow pins are guide sticks and the round connectors connect to the coax lines. The one used in this thesis is modified from this one. The large bus visible above the pins is sealed off, and the pins are female connectors.

3.2 Wiring and control electronics

THE qubit control is done by using arbitrary waveform generators; Tek AWG5014C. With this we are able to send truncated pulses out. By passing this signal through a Rohde & Schwarz SGS100A - a vector RF source, we can modulate the signal from the AWG to match respectively the cavity and the qubit frequency. They also gives us the capacity to apply out of phase pulses, using I-Q modulation, effectively creating the X and Y pulses.

To control the voltage gate, controlling the Josephson energy, we use a Keithley 2400, general purpose source meter.

The wiring is depicted in the appendix A1 in FigA.1. The two coax lines, Coax 13 and Coax 9 are for the qubit gate control. There are two gate-lines to accommodate for two-qubit devices. The bias-T's are functioning as a 20kHz lowpass, allowing the DC signal to only go down into the fridge. Flux bias lines is unused in this experiment. The line in, and line out, are for respectively driving, and reading out the signal. All white boxes a attenuators, with designated attenuation. All coax cables are either stainless steel or Niobium-Titanium, both superconducting in the *mk* environment.

3.3 Qubit device

The qubit device used is 2 qubit device, manufactured by Thorvald Wadum Larsen, designed to be 2 Gatemons, both with frequencies in the GHz scale.

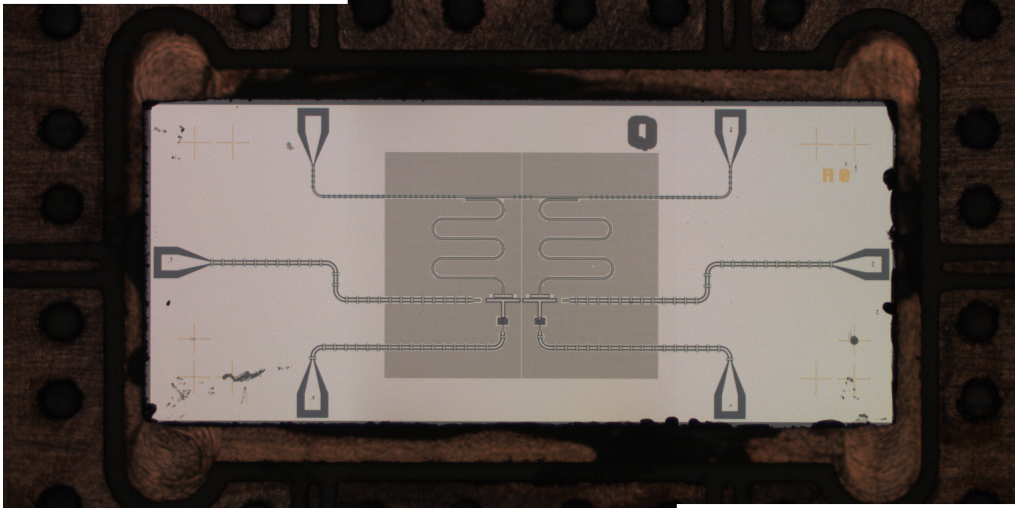


Figure 3.2: The Gatemon device, manufactured by Thorvald Larsen. Only the right qubit on the devices has been used in this thesis.

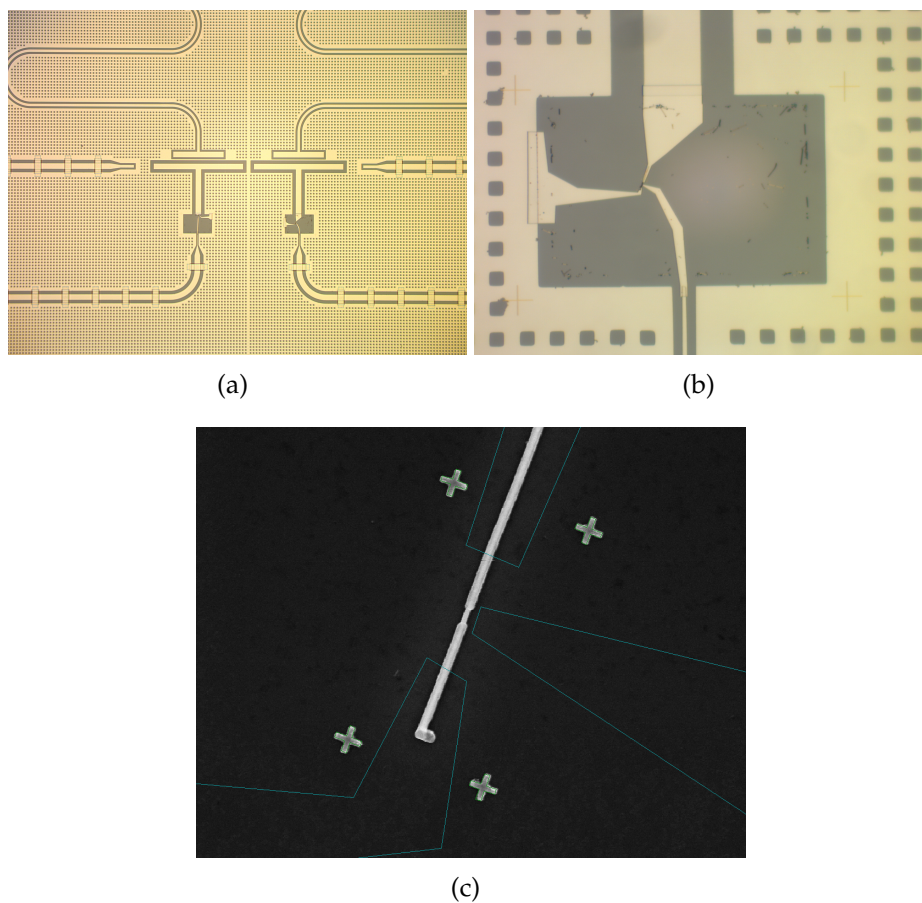


Figure 3.3: (a), We see on the right qubit the T-shaped superconducting island, the capacitively coupled cavity above the qubit, from the right the X and Y control, and at the bottom of the T, there is the gatecontrolled junction. (b) A zoom in on the junction. (c) A scanning electron micrograph of the etched InAs-Al nanowire. The etched region is 200nm long, and is visible by the distinctly thinner region.

4.1 Single qubit control (with microwaves)

FIRST and foremost, we see that the qubit is responsive. By sweeping the gate voltage, we see the highly non-linear dependency on the gate voltage. We see, that when changing the gate voltage, and therefore changing the qubit frequency, we change the amount of shift the cavity feels, as expected from Eq. 2.7.

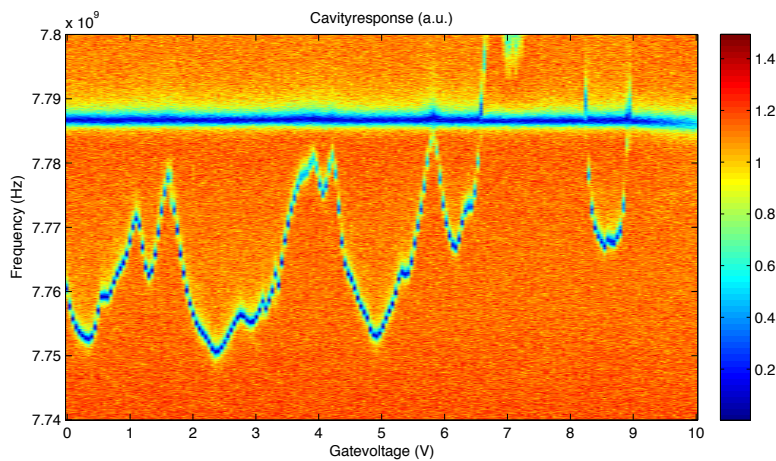


Figure 4.1: The wobbly line is the right cavity, as we sweep the right gate. The broad line at 7.7GHz is the left cavity, and is therefore unaffected by the sweep in voltage.

Driving the qubit on frequency gives us Rabi oscillations. The oscilla-

tions between the two states are clear, and seems to only depend on how long we apply the drive. That however, is only because the time scale is rather short; only 100ns. On longer time scales, dephasing and qubit life time dampen the oscillation.

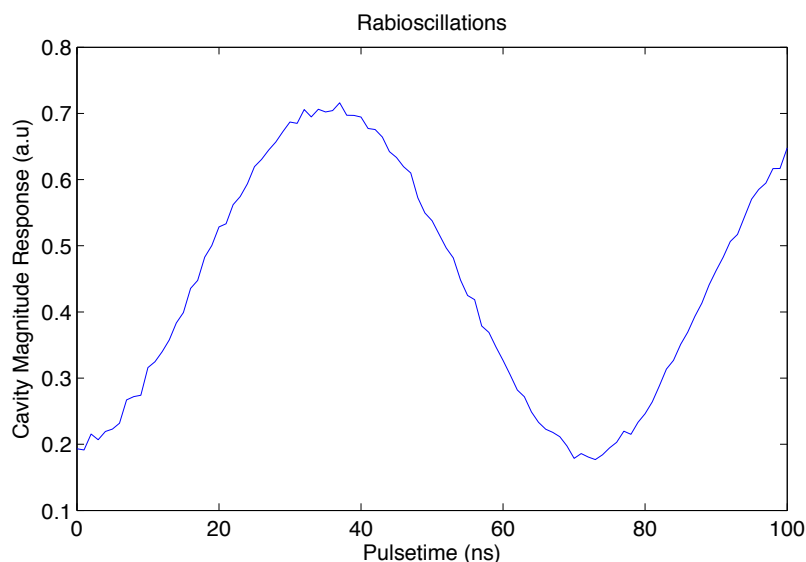


Figure 4.2: Rabi oscillations between ground and first excited stated. Since the magnitude of the cavity response depends on e.g. at exactly which frequency we measure the cavity, the magnitude doesnt tell us anything.

The Ramsey experiment also gives us the expected behaviour. The larger detuning of the qubit with higher gate voltage is evident, ranging from what seems to be nearly 0 detuning, to a detuning of $\approx 32\text{MHz}$. By doing even longer separation time, detuning of 1MHz can be detected, which is a very powerful tool when considering the relative precision: $f_q/\Delta \approx 50000$.

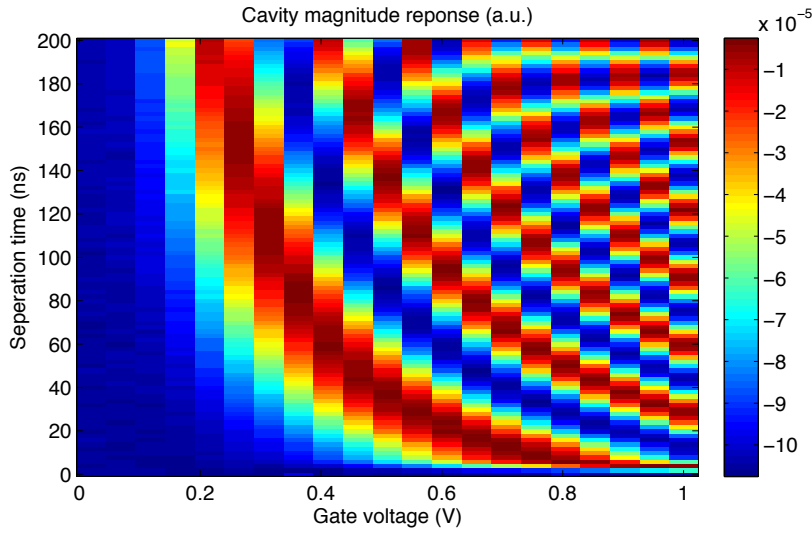


Figure 4.3: Ramsey oscillations between ground and first excited states. The qubit is driven at resonance at 0 gate voltage, and by applying the gate pulse for a time, we see the phase oscillations in the XY plane.

4.2 Randomized benchmarking

USING the random benchmarking using Clifford gates, we get overall error of the reference set. The fidelity of the reference is $p_{ref} = 0.967$. To obtain this data, 40 different random sequences have been measured for each point in Fig 4.4, the uncertainty on each being quite big, as seen in Fig 4.5, where all the data points for the reference has been plotted. It is similar for the interleaved gates, though here is only 20 measurements per point.

The individual errors is found by fitting the data points to eq. 2.10, and then use eq. 2.11 and eq. 2.12 respectively. The errors of the different gate are

Gate	Fidelity	Error
Identity	0.94 ± 0.01	$1.34\% \pm 0.9\%$
X	0.95 ± 0.02	$1.0\% \pm 0.9\%$
X/2	0.95 ± 0.01	$0.9\% \pm 0.7\%$
Y	0.96 ± 0.01	$0.8\% \pm 0.98\%$
Y/2	0.95 ± 0.01	$0.90\% \pm 0.9\%$

Now comparing the average Clifford gate with all the single qubit gates, is a bit unfair, as it gives off the feeling, that it must be all the other Clifford

gates that contributes the most. However, take into account that the average Clifford gate is 1.875 single gates, $1.65\%/1.875 = 0.8\% \pm 0.2\%$ per single qubit gate - being even lower than the Pauli gates. Even though the uncertainties are quite big, we are still near the fidelity threshold of 99% [2].

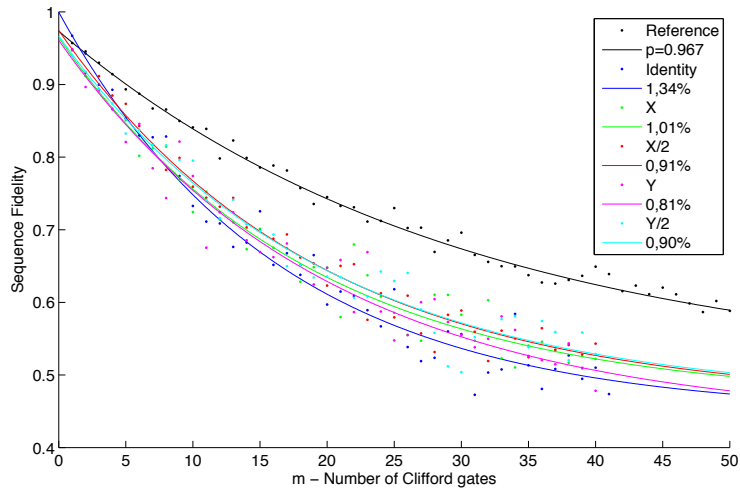


Figure 4.4: Interleaved Clifford sequences with the simplest gates, the Pauli gates. The reference is the Random Clifford without any interleaving gate. Noticeable larger noise on the Interleaved. This might be due, that every point is only meaned over half as many points as for the reference.

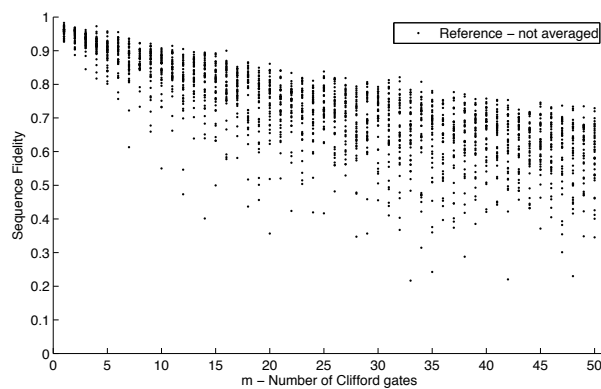


Figure 4.5: All the data points for the reference. A big spread towards the end is visible.

CONCLUSION AND LOOKOUT

 WITH an gate error around the fault tolerant threshold, we've shown that we've come far with this voltage-gate controllable qubit. As a first attempt, even though other groups as e.g. Martinis group, have managed gate fidelities of three nines, the gatemon is showing great potential, and we are catching up. Even though the numbers not yet allow me to proclaim, that we have made it, we are close.

Getting the rest of the gates characterized, and getting the measured Pauli gates even better, is ongoing work. Ways to tune the qubit not yet tested, and ongoing work of suppressing higher order transitions are sure to bring us more firmly into the fault tolerant fidelity regime.

These test were conducted one a single qubit, on a two qubit device. And of course, the two qubit interaction is one of our many next challenges. Also important is all the work that has been done, that is not mentioned in this thesis. This device is already leaps ahead of the single qubit device used in [?], and new devices just on our doorstep are believed to take us leaps ahead again.



APPENDIX

Triton 5 off-centre coax

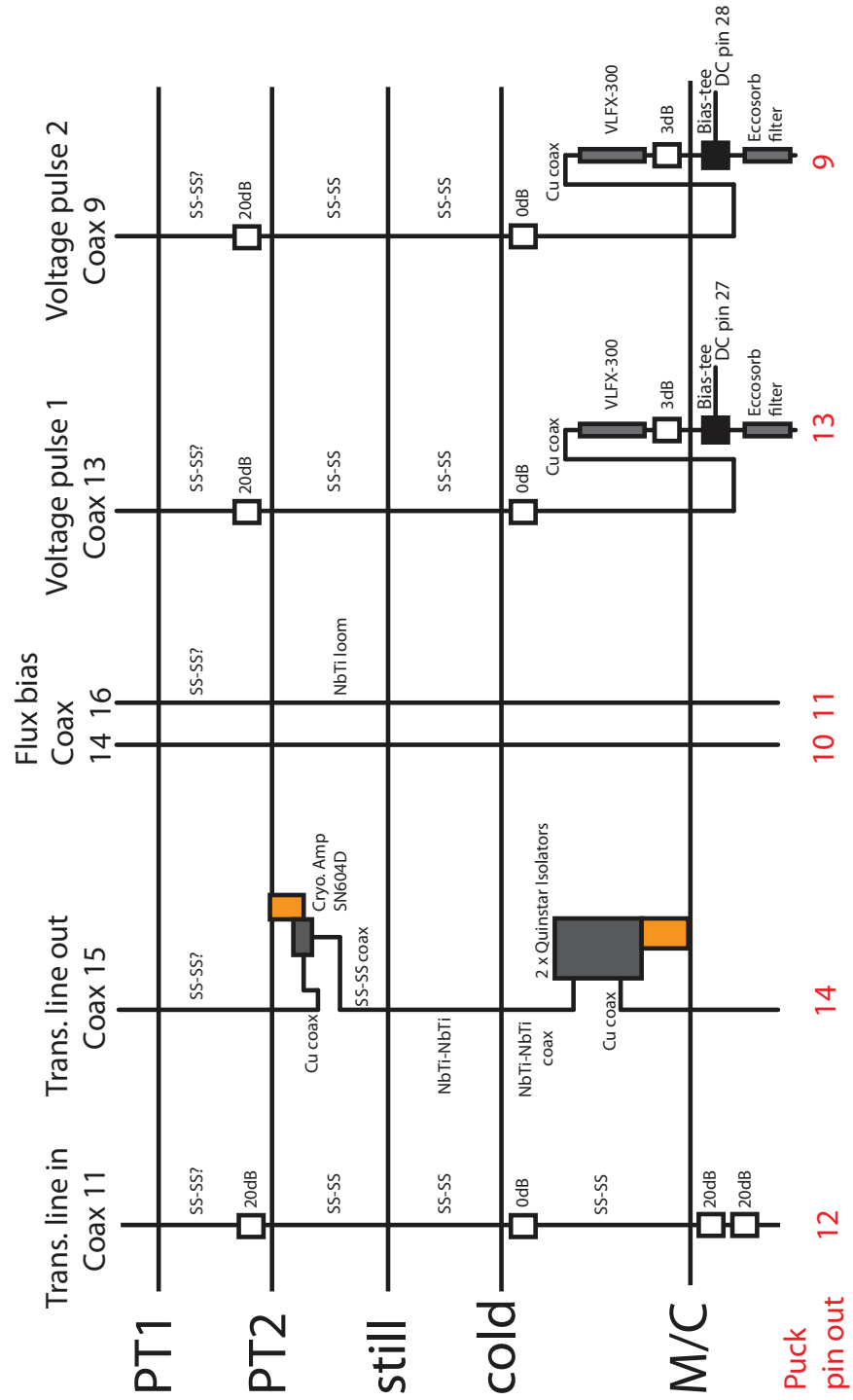


Figure A.1: The wiring inside the fridge

BIBLIOGRAPHY

- [1] The physical implementation of quantum computation.
- [2] R. Barends, J. Kelly, A. Megrant, A. Veitia, D. Sank, E. Jeffrey, T. C. White, J. Mutus, A. G. Fowler, B. Campbell, Y. Chen, Z. Chen, B. Chiaro, A. Dunsworth, C. Neill, P. O'Malley, P. Roushan, A. Vainsencher, J. Wenner, A. N. Korotkov, A. N. Cleland, and J. M. Martinis. Superconducting quantum circuits at the surface code threshold for fault tolerance. *Nature*, 508, Mar 2014.
- [3] J. M. Chow. *Quantum Information Processing with Superconducting Qubits*. Yale University, (2010).
- [4] J. M. Chow, J. M. Gambetta, L. Tornberg, J. Koch, L. S. Bishop, A. A. Houck, B. R. Johnson, L. Frunzio, S. M. Girvin, and R. J. Schoelkopf. Randomized benchmarking and process tomography for gate errors in a solid-state qubit. *Phys. Rev. Lett.*, 102:090502, Mar 2009.
- [5] C. Kittel. *Introduction to Solid State Physics (8th ed.)*. Wiley, (2014).
- [6] J. Koch, T. M. Yu, J. Gambetta, A. A. Houck, D. I. Schuster, J. Majer, A. Blais, M. H. Devoret, S. M. Girvin, and R. J. Schoelkopf. *Charge-insensitive qubit design derived from the Cooper pair box*. *Phys. Rev. A* 76, 042319, (2007).
- [7] T. W. Larsen, K. D. Petersson, F. Kuemmeth, T. S. Jespersen, P. Krogstrup, J. Nygard, and C. M. Marcus. *A Semiconductor Nanowire-Based Superconducting Qubit*. Not Published, (2015).
- [8] M. D. Reed. *Entanglement and Quantum Error Correction with Superconducting Qubits*. Yale University, (2013).
- [9] D. I. Schuster. *Circuit Quantum Electrodynamics*. Yale University, (2007).

- [10] D. H. Slichter. *Quantum Jumps and Measurement Backaction in a Superconducting Qubit*. University of California, Berkeley, (2011).